Supplementary Materials S2: Infrared Observational Data and Detection Protocols

Setup and Conditions:
Images were acquired using high-sensitivity infrared (IR) thermography under low-light indoor conditions. These observations serve as the primary empirical motivation for the phase-transition hypothesis and the material reorganization model proposed in the main text.

Supplementary Figure S1: Empirical Characterization of Decoupling

Figure S1: In-situ Observation of Recoil-Induced Ejection. Recorded on 2021-11-30.

- **Panel A (Phase A):** The entity is shown consolidated on the optical substrate (camera lens), exhibiting a stable thermal signature and surface adhesion.
- **Panel B (Phase B):** Captured at the frame immediately following the **Rayleigh-Newtonian recoil**. The entity is shown in mid-ejection, having generated sufficient internal mechanical force to overcome substrate adhesion.

Supplementary Figure S2: Time-Resolved Post-Ejection Navigation Sequence

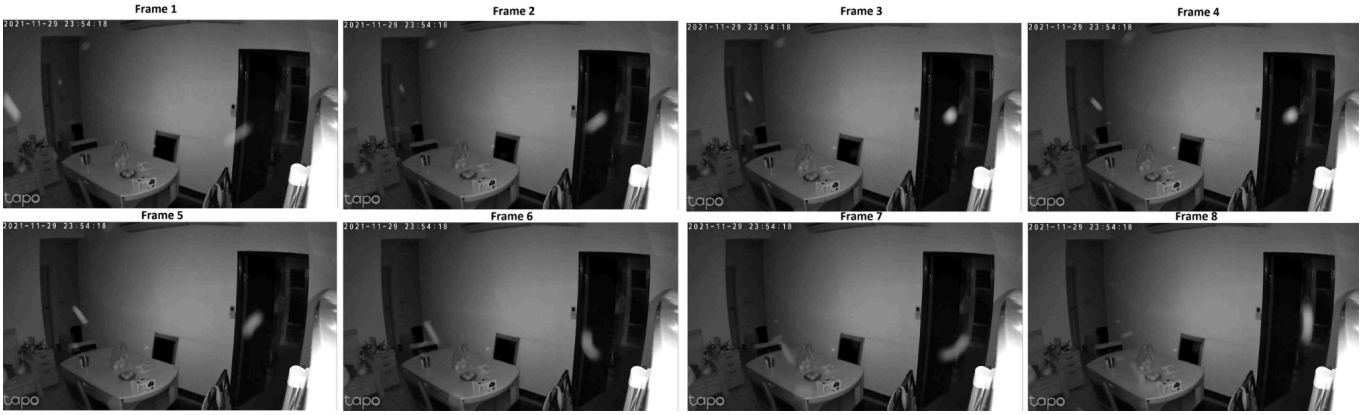

Figure S2: Kinematic Analysis of Autonomous Trajectory.

- **Temporal Resolution:** High-speed sequence captured at $\Delta t = 125\ \mathrm{ms}$ intervals.
- **Frame 1 (The Launch):** Demonstrates the initial ballistic impulse initiated by the Rayleigh instability mechanism.
- **Frames 2–8 (Active Navigation):** Illustrates the transition from purely ballistic momentum to autonomous translocation. The **non-linear path deviations** recorded here indicate active internal steering (modeled as protonic ruddering) rather than passive environmental drift or simple gravitational decay.

Analytical Correlation: ICP-MS Samples and Species Agnosticism

The micro-particulate matter subjected to **HR-ICP-MS elemental analysis** (as detailed in Table 1 of the main text) was recovered following observed departure and landing events identical to those documented in Figures S1 and S2. The chemical signature (+1154.3% Zn enrichment) is thus directly linked to the physical entities exhibiting these autonomous kinematic behaviors.

Analytical Limitation and Anonymity:
It is important to note that the current elemental analysis reflects the fundamental inorganic-organic convergence common to the mammalian neural extracellular matrix. Due to the highly conserved nature of these neurochemical precursors (specifically Zinc and Polyphosphates) across the mammalian class, **it is currently can't to predict or determine the specific mammalian species of origin for the recovered samples based on elemental fingerprints alone.** This "species-agnostic" characteristic emphasizes that the observed phenomenon is a generalized biophysical phase transition rather than a species-specific pathological event, ensuring the focus remains on the universal material dynamics of the SMQBP.

Field Observations and In-situ Detection Protocols

Empirical field surveys indicate that consolidated SMQBP entities demonstrate a preference for low-illuminance, subterranean structures (e.g., underground parking facilities), likely to minimize external electromagnetic interference and maintain lattice coherence.

- **UV Detection Protocol:** A **Photophobic Kinetic Response** is triggered by exposure to high-intensity ultraviolet radiation ($\lambda = 395\ \text{nm}$, Power $> 50\ \text{W}$).
- **Proposed Mechanism:** Exposure to 395 nm photons is hypothesized to induce **electronic instability** within the Zn-sHA semiconductor lattice. This energy saturation forces the entity to manifest visually and initiate rapid evasive translocation, which facilitates the high-speed optical documentation of the transition.